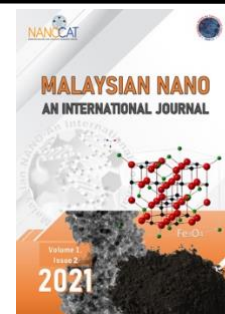




## Malaysian NANO-An International Journal



### Research Article

## TLM Analysis of Metal Contacts for 2D MoS<sub>2</sub> Nanoflakes Deposited by Chemical Vapour Deposition-free technique

Received 15<sup>th</sup> September 2021  
Revised 9<sup>th</sup> November 2021  
Accepted 28<sup>th</sup> November 2021

DOI:

<https://doi.org/10.22452/mnij.vol1no2.3>

Corresponding authors:

rozalina@um.edu.my,  
cheelong@gmail.com

A.H. Abdullah Ripain<sup>a</sup>, C.L. Tan<sup>a\*</sup>, R. Zakaria<sup>a\*\*</sup>

<sup>a</sup>University of Malaya- Photonics Research Centre, Faculty Science, University of Malaya, 50603, Kuala Lumpur, Malaysia

### Abstract

In the past decade, two-dimensional (2D) nanomaterials are gaining significant attention due to their novel properties in electrical, optical, mechanical which are different from their bulk forms. Therefore, it becomes one of the most promising materials for sensing applications. However, to connect the 3D world with 2D materials require excellent communication links which is a contact that renders remarkable electrical properties and specifically 2D nanomaterials-based sensor has been suffering from high resistance and low sensitivity due to the loss caused by poor contact between the 2D nanomaterials and metal interface. This work explores the electrical properties of metal/2D contacts by the rectangular transmission line method (TLM). The critical resistance parameters such as sheet and specific contact resistance were determined by characterizing the current-voltage (IV) relation. The behavior of different metals (silver and gold) contacts to 2D MoS<sub>2</sub> nanoflakes deposited on Si substrate by low-cost spray coating technique are observed. These metals are chosen based on the work function relative to the electron's affinity,  $\chi$  of MoS<sub>2</sub>. UV-Vis's analysis is carried out to estimate the final concentration of MoS<sub>2</sub> solution.

**Keywords:** 2D; MoS; Nanoflakes; Chemical vapor deposition

## 1. Introduction

Low-dimensional nanomaterials are among the first choices for the design of sensor materials, due to their unique properties that are derived from their quantum size effect and surface effect [1-3]. Among low-dimensional nanomaterials, two dimensional (2D) nanomaterials, including graphene and transition metal chalcogenides (TMDCs), are excellent examples [4]. The most studied material of TMDCs family is molybdenum disulphide ( $\text{MoS}_2$ ) because of its robustness along with the tungsten selenide ( $\text{WSe}_2$ ). Both  $\text{MoS}_2$  and  $\text{WSe}_2$  are semiconductors in stable 2H phase and reducing the thickness from the bulk layer to monolayer, it is found that the transition indirect-to-direct band gap had occurred [5].

2D  $\text{MoS}_2$  has been applied in many devices including field-effect transistors (FETs), photodetectors as well as electrochemical applications [6-8]. All these electronics applications rely on electronics contacts to operation. Due to that reason, understanding metal/2D  $\text{MoS}_2$  semiconductors is crucial. These metal-semiconductor contacts are an indispensable part of a semiconductor-based device that can behave either Schottky barrier or as an Ohmic dependent on the characteristic of the interface. These are delineated by electrical parameters such as specific contact resistivity ( $\rho_c$ ), sheet resistance ( $R_{sh}$ ) and contact resistance ( $R_c$ ). Nanoengineering and measurement of these parameters are significantly growing in 2D semiconductor materials industry and to lower the contact resistance of the metal/2D nanomaterials various techniques have been studied. All the resistance parameters are important to determine prior to any optoelectronics devices using TLM measurement.

In this work, a detailed experimental analysis of metal/2D  $\text{MoS}_2$  nanoflakes contact with different metals are conducted. As reported, the lower metal work functions of the contacts can lead to smaller Schottky barrier height and resistances [9]. The metals in this letter are chosen based on the work functions relatively to the electron's affinity,  $\chi$  of  $\text{MoS}_2$  (4.0 eV). Relatively low metal work functions,  $\Phi_m$  silver (4.33 eV) is studied along with relatively high metal work function, gold (5.4 eV) to give a wide picture of TLM analysis of metal/2D  $\text{MoS}_2$  contact

## 2. Materials and Methods

A solution of  $\text{MoS}_2$  was prepared for spray coating deposition on Si substrate. In brief,  $\text{MoS}_2$  powder (99% purity, Sigma Aldrich) was mixed with a solvent mixture of ethanol and deionized (DI) water at a ratio of 9:11 to exfoliate into a thinner layer and immediately refined with high power bath sonication (GT Sonic Model: VGT-1620QTD) for 8 hours to form a stable and uniform solution.

The supernatant of MoS<sub>2</sub> was collected after centrifugation for 20 minutes at 233 g. UV-Vis measurement was made on the MoS<sub>2</sub> solution to estimate the final concentration. Substrates were all cleaned with (in order of) acetone, iso-propanol solution, distilled water for 10 minutes each. The samples are then dried using Ni gas. The MoS<sub>2</sub> solution was deposited on Si substrate via spray-coating deposition with a controlled volume of 4ml for each sample as shown in Figure 1. The Si substrate was heated at 150°C for 15 minutes on a hotplate before the spraying process to facilitate solvent evaporation. The pressure and distance of spray nozzle from the sample were 21 psi and 20 cm respectively. All the parameters are kept constant during the process.

The metal contact was prepared after the MoS<sub>2</sub> thin film deposition. A TLM mask with metal pad distance separation,  $d_i$  in the range between 0.5 to 1.3 mm was placed on top of the sample and metals electrodes (Ag and Au) was deposited by electron evaporation beam (e beam) at  $\sim 1 \text{ \AA}$  deposition rate under a pressure of  $1 \times 10^{-6}$  Torr, respectively. The thickness of the Ag and Au layer was 100 nm. The fabricated devices have same effective contact area ( $1 \times 1.5 \text{ cm}^2$ ) namely the area of p-Si covered by MoS<sub>2</sub> thin film.

TLM measurement was conducted under ambient conditions and the dark currents were measurement in a dark box to eliminate the interference of ambient light using two-point-probe method. Current-Voltage (IV) curve was precisely obtained using Keithley source meter (2410) with potential scanning from -1.5 to 1.5 V, where the current was measured through two successive metal pads distance,  $d_i$ , keeping a constant voltage across the contacts as shown in Figure 2. The total resistance,  $R_T$  between the metal-semiconductor-metal ( $R_{T1}$ ,  $R_{T2}$ ,  $R_{T3}$ , ...) was determined from the reciprocal of the IV curve gradient.

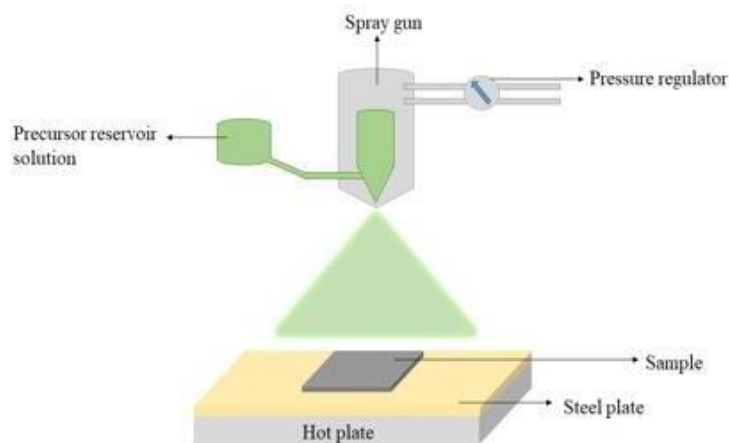


**Figure 1:** Schematic representation of spray-coating process

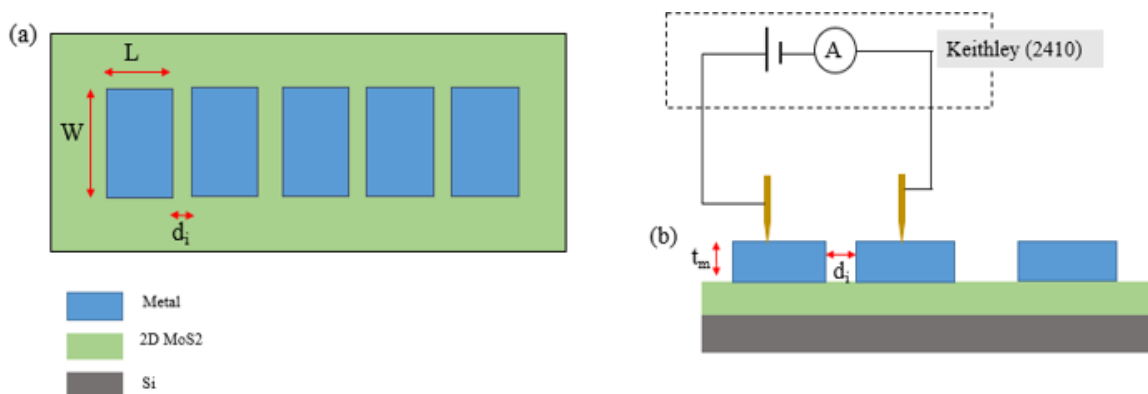


**Figure 2:** Schematic diagram of a) TLM test structure (top view) b) current-voltage measurement on samples.

### 3. Results and discussion

#### 3.1 Synthesis of MoS<sub>2</sub>: Concentration and UV-Vis Analysis

The 2D MoS<sub>2</sub> nanoflakes used in this work are prepared using a liquid exfoliation technique similar to that reported by Zhou *et al* [10]. Two volatile and low-boiling point solvents; ethanol and water are used in the preparation MoS<sub>2</sub> solution. The dispersion of 2D nanomaterials can be partially predicted by Hansen solubility parameters (HSP) theory [11, 12]. Three HSP parameters used are  $\delta_D$ ,  $\delta_P$ ,  $\delta_H$  which are dispersive, polar and hydrogen bonding solubility parameters, respectively. The level of adaption between the HSP of solvents and MoS<sub>2</sub> is determined by the value of distance  $R_a$ . Higher solubility is expected if the  $R_a$  value smaller [10]. According to the previous work, the smallest  $R_a$  for MoS<sub>2</sub> is obtained with a mixture of ethanol and water at a 9:11 ratio. Figure 3 shows the schematic illustration of MoS<sub>2</sub> synthesis and photographs of MoS<sub>2</sub> which have been stored under ambient conditions after a few weeks. Color remains unchanged and no precipitation occurred indicate the stability and no degradation in MoS<sub>2</sub> solution.

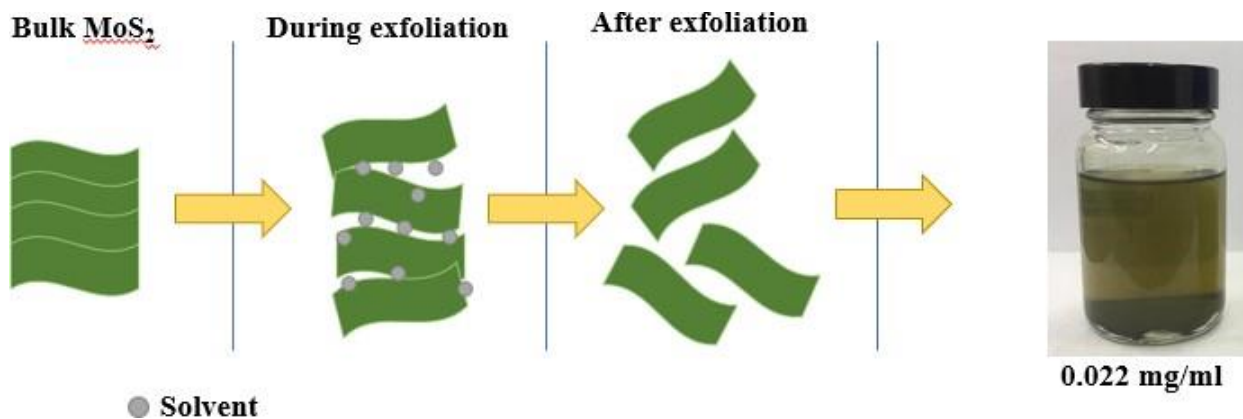


**Figure 3:** Schematic illustration of MoS<sub>2</sub> synthesis and photographs of MoS<sub>2</sub>

UV-Vis analysis was carried out to find the final concentration 2D MoS<sub>2</sub> solution. The estimation of the concentration is based on the Beer-Lambert Law equation [13]

$$A = a_{\lambda}cl \quad (1)$$

Where  $a_{\lambda}$ , is optical absorption coefficient, concentration and length of the light passes respectively. UV-Vis absorption spectrum for MoS<sub>2</sub> dispersion in ethanol/water mixture is shown in Figure 4.

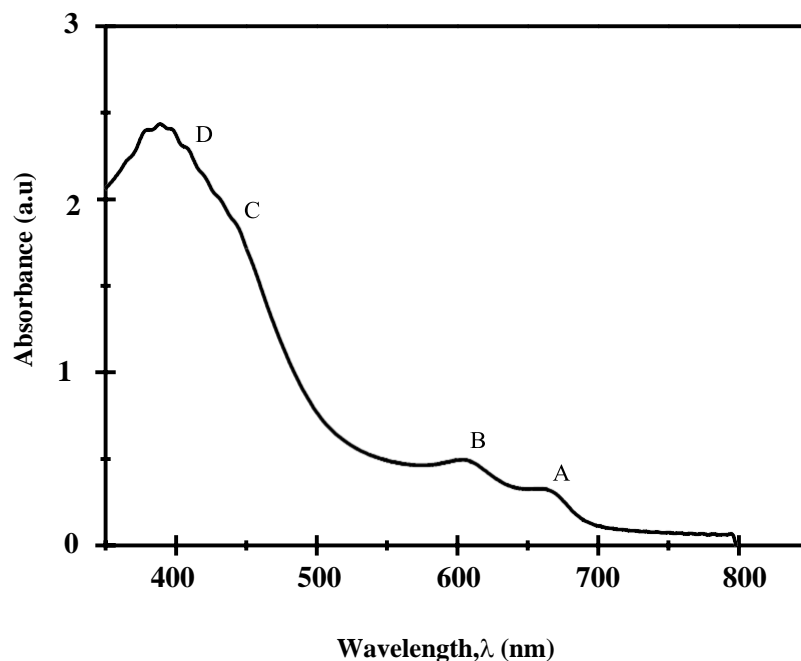


**Figure 4:** UV-Vis absorption spectrum of MoS<sub>2</sub>

There are four significant peaks; peak A (~667 nm) and peak B (~605 nm) are from excitonic transitions while peak C (~442 nm) and D (~408 nm) are due to the transitions between the higher density state regions of band structure [14, 15]. Following the Beer-Lambert Law, using optical absorption coefficient for MoS<sub>2</sub>  $\alpha_{672} \sim 1268 \text{ Lg-1m-1}$  [12, 13] the estimation concentration is 0.022 mgml<sup>-1</sup>. The concentration in this work is close to the value reported by Zhou et al [10]. Hence, this proved that two ‘poor’ solvents ethanol and water can be designed to give high dispersion and good stability in MoS<sub>2</sub>.

### 3.2 Electrical Characterization: Current-Voltage Measurement and TLM Analysis

In an attempt to study the properties of metals when in contact with 2D MoS<sub>2</sub> nanoflakes, two different metals; silver and gold with different work functions are considered. Figure 5 illustrates the band alignment of metal and MoS<sub>2</sub> before and after in contact for the case of metal work function,  $\Phi_m$  greater than MoS<sub>2</sub> electron affinity,  $\chi$  which is valid for both metals in this work. In order to achieve the equilibrium state; the Fermi levels of two materials are coexisted, conduction and valence band of the semiconductor bend towards the Fermi level of metal. Assuming the MoS<sub>2</sub> is an n-type semiconductor with a lower work function than metal, the electrons diffuse from semiconductor to metal. As a result of electrons flow to the metal, a negative charge builds up at the surface of the metal side and a positive charge at the semiconductor causing a formation of the electric field in the gap between metal and semiconductor. Consequently, the electrons need to pass a barrier upon returning to the semiconductor, which is known as Schottky barrier,  $\Phi_{SB}$ . The barrier value is estimated using Schottky-Mott rule ( $\Phi_{SB} = \Phi_m - \chi$ ). Higher metal work function gives out higher  $\Phi_{SB}$ . Hence Au/MoS<sub>2</sub> has higher  $\Phi_{SB}$  than Ag/ MoS<sub>2</sub> as work function Ag is lower than Au. A larger forward bias is required to overcome this barrier. This is confirmed from the current-voltage (I-V) curve in Figure 5 as it can be seen that the current is slightly higher for Au under identical bias conditions indicating the charge transmission capabilities for Au/MoS<sub>2</sub> interface at room temperature. IV curve results in nearly symmetric, non-linear characteristic possibly due to Schottky barrier at contacts. The estimated Schottky barrier is shown in Table 1.

**Table 1:** Experimental results of different metal/2D MoS<sub>2</sub>

<i>Metals</i>	<i>Work function, <math>\Phi_m</math> (eV)</i>	<i>Schottky barrier, <math>\Phi_{SB}</math> (eV)</i>	<i>Current at +1.5 V bias (<math>\mu A</math>) at smallest <math>d_i</math></i>
<i>Ag</i>	4.33	0.33	2.21
<i>Au</i>	5.4	1.4	2.71

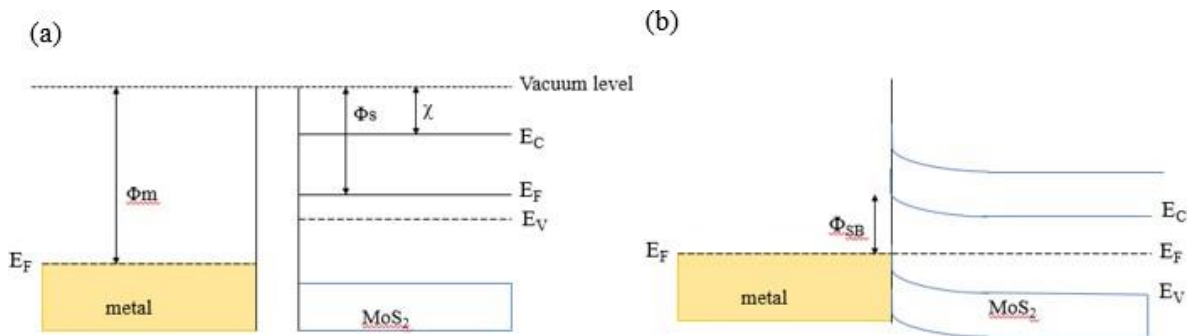


**Figure 5:** Band alignment of metal and semiconductor MoS<sub>2</sub> a) before b) after in equilibrium state.

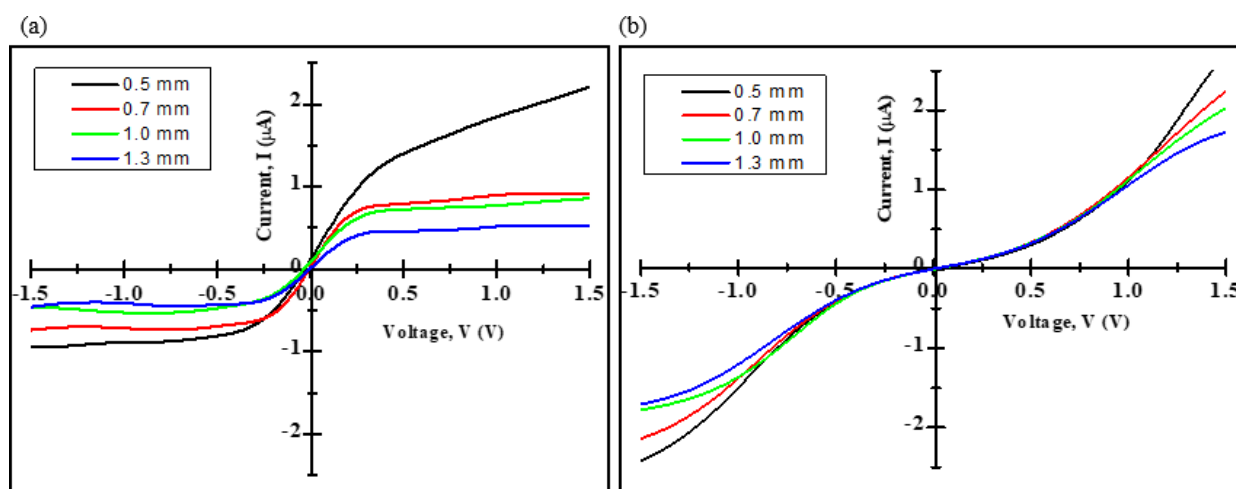


**Figure 6:** IV characteristic for different metals a) Ag b) Au under identical bias -1.5 to 1.5 V

Figure 6 shows the IV curve at room temperature corresponding to the metal pads separation,  $d_i$  (0.5, 0.7, 1.0, 1.3) mm of two different metals; silver and gold on 2D MoS<sub>2</sub> thin films. Total resistance,  $R_T$  determine by the reciprocal of the gradient. Graph total resistance,  $R_T$  against metal separation pad,  $d_i$  has been plotted for both samples at forward and reverse bias. Figures 7 and 8 portrayed the total resistances versus metal pad separation,  $d_i$  for both silver and gold contact at forward and reverse bias.

As shown in Figure 1 (b),  $R_T$  between any two consecutive contacts can be expressed as a linear combination of  $R_C$  and the  $R_{SH}$  i.e.:

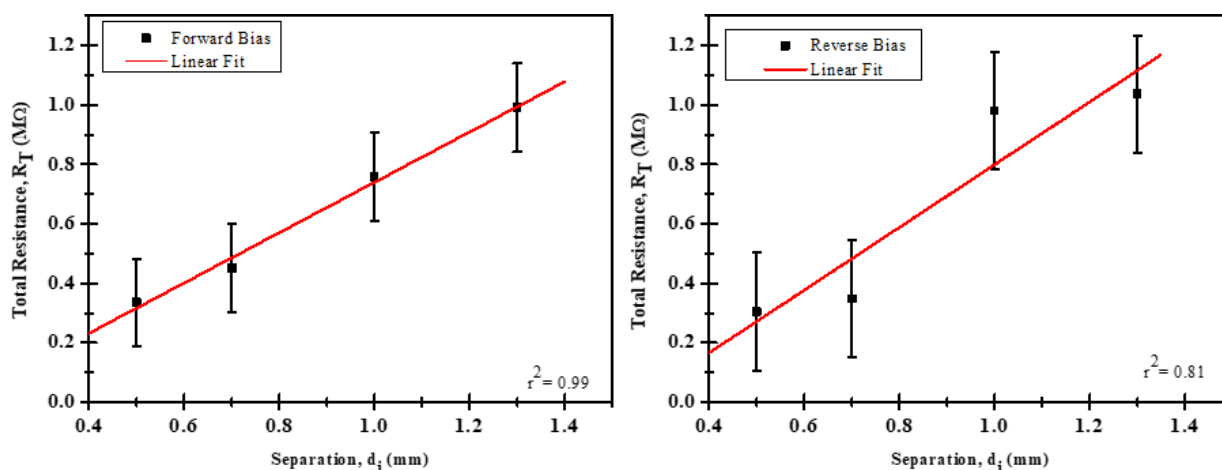
$$R_T = R_{SH} \left( \frac{L}{W} \right) + 2R_C \quad (2)$$

RC is extracted by finding the y-intercept using linear fit in Figures 6 and 7 for each sample and RSH is the resistance of semiconductor thin film between the two contacts which can be obtained from the slope of the RT versus di plot multiply by the width of the metal pads, W. It can be seen that Au/MoS<sub>2</sub> contact showed lower sheet and contact resistance which are 0.09 kΩ/sq and 197.47 kΩ mm respectively than Ag/MoS<sub>2</sub> contact. This showed that electron transmission across the Au/MoS<sub>2</sub> contact is better than in Ag/MoS<sub>2</sub>. The value of RC obtained in this work is quite higher than previously reported work [16, 17] as no special interlayer is inserted as a protection layer of metal in the sample structure that leads to contamination and a higher value of RC.

As a point of comparison, a standard quantity is preferred in making different contact. The contact resistance depends on the size of the contact; hence it is not a good point of comparison. Instead, the specific contact resistance, ρ<sub>c</sub> is required. The specific contact resistance, ρ<sub>c</sub> = RC AC where RC and AC are resistance associated with the metal/semiconductor interface and contact area respectively. Finding its value is not straightforward as the current flow into the contact is not uniform thus current transfer length, L<sub>T</sub> is introduced. The transfer length is also known as effective length is the average distance that an electron/hole travels in the semiconductor beneath the contact before it flows up into the contact. The transfer length can be obtained from the graph by extrapolating back to the horizontal axis in Figures 7 and 8. Using the value of transfer length for each contact, specific contact resistance is possible to measure by the equation as follow:

$$\rho_c = R_{SH} \times L_T^2 \tag{3}$$

Ag/MoS<sub>2</sub> contact gives out the lowest specific contact resistance value (17.02 Ω.mm<sup>2</sup>), while



Au/MoS<sub>2</sub> contact shows the highest value (107.92 Ω.mm<sup>2</sup>) under identical bias. Table 2 summarized the experimental results of resistance parameters obtained using two different metals contacts under forward and reverse bias.



**Figure 7:** Total resistance,  $R_T$  against metal pad separation,  $d_i$  for Ag/MoS<sub>2</sub> contact at a) forward b) reverse bias.

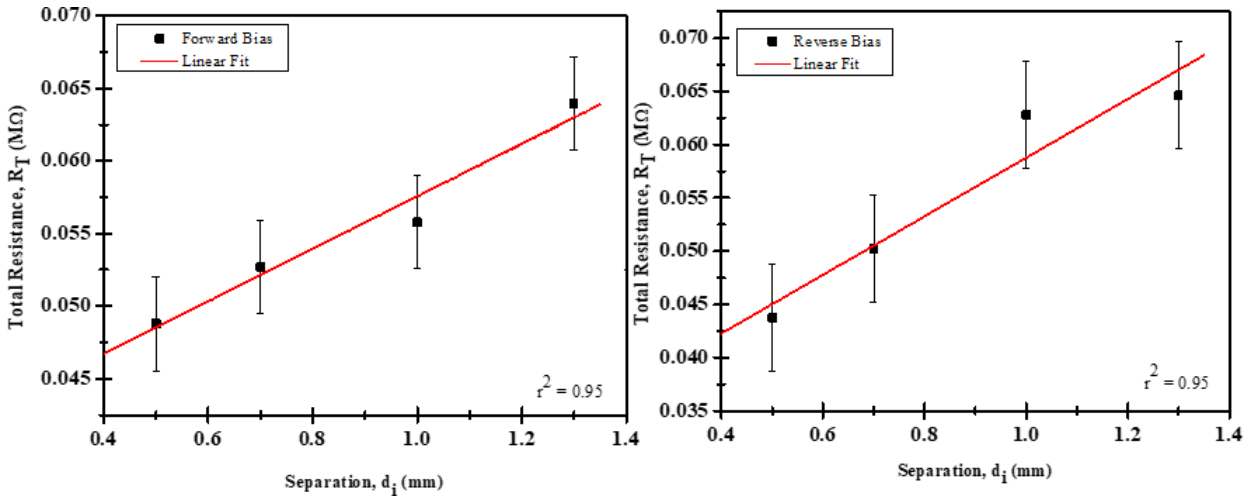


**Figure 8:** Total resistance,  $R_T$  against metal pad separation,  $d_i$  for Au/MoS<sub>2</sub> contact at a) forward b) reverse bias.

**Table 2:** Resistance parameters obtained using two different metals contacts under forward and reverse bias.

METAL	Bias	Sheet resistance, $R_{SH}$ (kΩ/sq)	Contact resistance, $R_c$ (kΩ-mm)	Specific contact resistance, ( $\Omega$ -mm <sup>2</sup> )	Current transfer length, $L_T$ (mm)
Ag	Forward	4.24	537.01	17.02	0.06
	Reverse	5.28	1282.40	77.89	0.12
Au	Forward	0.09	197.47	107.92	1.09
	Reverse	0.14	156.34	44.43	0.57

#### 4. Conclusion

In summary, we can produce MoS<sub>2</sub> solution by liquid exfoliation technique using two poor solvents and deposit the solution by low-cost spraying method on the substrate. UV-Vis analysis was made to estimate the final concentration of the solution which is 0.022 mgml<sup>-1</sup>. By TLM analysis, we investigated the properties of metal/2D MoS<sub>2</sub> contacts using two different metals, silvers and gold which work functions are relatively lower than the electron affinity of MoS<sub>2</sub>. Both metal contacts showed Schottky behavior. We measured the value of specific contact resistance for Ag/MoS<sub>2</sub> and Au/MoS<sub>2</sub> which are 17.02  $\Omega$ .mm<sup>2</sup> and 107.92  $\Omega$ .mm<sup>2</sup> respectively. Thus, the Ag/MoS<sub>2</sub> has lower specific contact resistance than Au/MoS<sub>2</sub> contact under identical bias.

TLM analysis holds some severe limitations in analyzing non-linear IV curves for Schottky contacts as contact resistance,  $R_c$  becomes bias-dependent, which requires careful consideration when examining scaling behavior. The effect of this nonlinearity in the plot of total resistance,  $R_T$  against the metal pad separation,  $d_i$  is difficult when extracted transfer length,  $L_T$  is small. In addition, some assumption needs to be made; sheet resistance under the contact is the same as sheet resistance between the contact that allows us to extract  $L_T$  by finding the x-intercept of curve  $R_T$  versus  $d_i$ .

### Competing interest

The authors declare no conflict of interest.

### Acknowledgments

The authors acknowledge support from members of Plasmonic Lab, Photonic Research Centre, University of Malaya with project funding under University of Malaya Impact-Oriented Interdisciplinary Research Grant Programme (IIRG), project code IIRG013C-2019.

### References

- [1] L. Cui, J. Wu, and H. Ju, Electrochemical sensing of heavy metal ions with inorganic, organic and bio-materials. *Biosensors and Bioelectronics*. 2015: 63; 276-286.
- [2] Du, X.-L., et al., An electrochemiluminescence sensor based on CdSe@ CdS functionalized MoS<sub>2</sub> and hemin/G-quadruplex-based DNAzyme biocatalytic precipitation for sensitive detection of Pb (ii). *Analytical methods*. 2018: 10(1); 51-58.
- [3] Z. Guo., et al., Simultaneous determination of trace Cd (II), Pb (II) and Cu (II) by differential pulse anodic stripping voltammetry using a reduced graphene oxide-chitosan/poly-l-lysine nanocomposite modified glassy carbon electrode. *Journal of colloid and interface science*. 2017: 490; 11-22.
- [4] Y. Sun., et al., Ultrathin two-dimensional inorganic materials: new opportunities for solid state nanochemistry. *Accounts of chemical research*. 2015: 48(1); 3-12.
- [5] O. Lopez-Sanchez., et al., Ultrasensitive photodetectors based on monolayer MoS<sub>2</sub>. *Nature nanotechnology*. 2013: 8(7); 497.
- [6] T.N. Walter., et al., Nickel diffusion into MoS<sub>2</sub> and the effect of annealing on contact resistance. *Materials Science in Semiconductor Processing*. 2020: 107; 104850.

- [7] Y. Zhang., et al., Fermi-Level Pinning Mechanism in MoS<sub>2</sub> Field-Effect Transistors Developed by Thermionic Emission Theory. *Applied Sciences*. 2020: 10(8); 2754.
- [8] A.K. Singh., et al., 2D layered transition metal dichalcogenides (MoS<sub>2</sub>): synthesis, applications and theoretical aspects. *Applied Materials Today*. 2018: 13; 242-270.
- [9] S. Walia., et al., Characterization of metal contacts for two-dimensional MoS<sub>2</sub> nanoflakes. *Applied Physics Letters*. 2013: 103(23); 232105.
- [10] K.G. Zhou., et al., A mixed-solvent strategy for efficient exfoliation of inorganic graphene analogues. *Angewandte Chemie*. 2011: 123(46); 11031-11034.
- [11] C.M. Hansen., Hansen solubility parameters: a user's handbook. *CRC press*. 2007.
- [12] J.N. Coleman., et al., Two-dimensional nanosheets produced by liquid exfoliation of layered materials. *Science*. 2011: 331(6017); 568-571.
- [13] G. Hu., Printable 2D Material Optoelectronics and Photonics, in Department of Engineering. 2017: University of Cambridge: 196.
- [14] A. Beal., J. Knights, and W. Liang, Transmission spectra of some transition metal dichalcogenides. II. Group VIA: trigonal prismatic coordination. *Journal of Physics C: Solid State Physics*. 1972: 5(24); 3540.
- [15] Y. Li., et al., Measurement of the optical dielectric function of monolayer transition-metal dichalcogenides: MoS<sub>2</sub>, MoSe<sub>2</sub>, WS<sub>2</sub>, and WSe<sub>2</sub>. *Physical Review B*. 2014: 90(20); 205422.
- [16] Y. Wang., et al., Van der Waals contacts between three-dimensional metals and two-dimensional semiconductors. *Nature*. 2019: 568(7750); 70-74.
- [17] R. Kappera., et al., Phase-engineered low-resistance contacts for ultrathin MoS<sub>2</sub> transistors. *Nature materials*. 2014: 13(12); 1128-1134.